Available online at www.sciencedirect.com

ScienceDirect

www.journals.elsevier.com/journal-of-environmental-sciences

JOURNAL OF ENVIRONMENTAL SCIENCES
www.jesc.ac.cn

Effects of surfactants on graphene oxide nanoparticles transport in saturated porous media

Wei Fan[1], *Xuehui Jiang*[1], *Ying Lu*[2], *Mingxin Huo*[1], *Shanshan Lin*[1,*], *Zhi Geng*[1]

1. *School of Environment, Northeast Normal University, Changchun 130117, China. Email: fanw100@nenu.edu.cn*
2. *Key Laboratory of Groundwater Resources and Environment, Ministry of Education, Jilin University, Changchun 130021, China*

ARTICLE INFO

Article history:
Received 1 December 2014
Revised 26 January 2015
Accepted 9 February 2015
Available online 28 May 2015

Keywords:
Graphene oxide
Porous media
Transport
Surfactants
Numerical modeling
DLVO

ABSTRACT

Transport behaviors of graphene oxide nanoparticles (GONPs) in saturated porous media were examined as a function of the presence and concentration of anionic surfactant (SDBS) and non-ionic surfactant (Triton X-100) under different ionic strength (IS). The results showed that the GONPs were retained obviously in the sand columns at both IS of 50 and 200 mmol/L, and they were more mobile at lower IS. The presence and concentration of surfactants could enhance the GONP transport, particularly as observed at higher IS. It was interesting to see that the GONP transport was surfactant type dependent, and SDBS was more effective to facilitate GONP transport than Triton X-100 in our experimental conditions. The advection–dispersion–retention numerical modeling followed this trend and depicted the difference quantitatively. Derjaguin–Landau–Verwey–Overbeek (DLVO) interaction calculations also were performed to interpret these effects, indicating that secondary minimum deposition was critical in this study.

Introduction

Graphene oxide (GO) is an oxidized form of graphene-based nanomaterials, featuring fascinating nanostructure with hydroxyl and epoxy bridge functional groups on the basal plane and carbonyl and carboxyl groups on the edges (Dreyer et al., 2010). These abundant hydrophilic O-functional groups on the surfaces were useful in synthesizing GO hybrids and composites, and then maximize the benefit of the unique properties in different applications (e. g. electronic, medical and environmental sectors) (Srivastava et al., 2014; Zhang et al., 2014). However, recent studies found that GO would be the most toxic graphene-based nanomaterial due to its considerable water solubility and noticeable cell damage. Exposures to GO might induce severe cyto-toxicity and lung diseases (Wang et al., 2011; Ahmed and Rodrigues, 2013). Increased applications and production of GO will likely lead to its release in the environment (such a as landfill leachate and wastewater infiltration) (Novikov et al., 2006; Hennebert et al., 2013), therefore, research attention should be dedicated to investigate the fate and transport of such an emerging materials for the public health concerns.

The threat extent of graphene oxide nanoparticles (GONPs) to the environment and public health is correlated to their ability to remain dispersed in the environment or to form particle aggregations, and consequently their mobility (Petosa et al., 2010; Ju-Nam and Lead, 2008). Nanoparticles with high mobility probably penetrate the soil layers and enter ground

* *Corresponding author*. E-mail: linss071@nenu.edu.cn (Shanshan Lin).

http://dx.doi.org/10.1016/j.jes.2015.02.007

water system, which posed potential risks for drinking water (Hennebert et al., 2013; Saito et al., 2013). Researchers suggested that the mobility and retention of GONPs in saturated porous media packed in columns were controlled by complexity of the porous media matrix (*e.g.*, grain surface, moisture content) (Liu et al., 2013a,b), the physicochemical parameters of solution chemistry (*e.g.*, ionic strength, pH and the presence of natural organic matter) (Feriancikova and Xu, 2012; Lanphere et al., 2013), and the fluid dynamics characteristic of the column system (Liu et al., 2013a; Qi et al., 2014). Although progress has been made towards a better understanding of the environmental fate and transport of GONPs, the current knowledge of the fate and transport of GONPs in porous media is far from complete. This is particularly true for the influence of other coexisting compounds in solution. To our knowledge, no research has been conducted to examine the effect of surfactants on the transport behavior of GONPs in saturated systems. Surfactants are widely present in water environments with the concentration even up to several thousand mg/L in municipal wastewaters (Adak et al., 2005), and it can likely coexist with the released GONPs during accidental infiltration or artificial groundwater recharge. Due to their surface-active properties, surfactants may adsorb to GONPs and affect their solubility and transport in porous media by modifying the particle surface chemistry and changing their interactions (Tkachenko et al., 2006; Lin et al., 2010).

The objective of this work was thus to examine the influence of surfactant on GONP transport through saturated porous media, and therefore obtain insight into the mechanism of mediated transport by coexisting compounds. The approach focused on a systematic identification of the mechanisms for enhanced transport of GONPs through sand columns with surfactants. The GONP transport experiment results were interpreted through surface property measurement of sand and GONPs, breakthrough curve (BTC) monitoring, numerical modeling and Derjaguin–Landau–Verwey–Overbeek (DLVO) theory.

1. Materials and methods

1.1. Porous media

Quartz sand was used as the porous medium with a size range of 0.36–0.50 mm and average diameter (d_{50}) of 0.42 mm. The sand was treated sequentially by 10% nitric acid (V/V) to remove metal oxides, and then 10% peroxide to eliminate organic materials. Subsequently, the sand was repeatedly rinsed with deionized (DI) water until a neutral pH (7.1 ± 0.1 finally) was achieved and water conductivity reduced to zero. The sand was dried in an oven at 110°C for 48 hr.

1.2. Graphene oxide

GO was purchased from Institute of Coal Chemistry, Chinese Academy of Sciences, which was synthesized by a pressurized oxidation method described by Bao et al. (2012). According to the manufacture, the GONPs had an average height of 0.7 ± 1.2 nm, and an average perimeter of 781.1 ± 502.2 nm. The GONP stock solution used in this study was prepared at 20 mg/L, and all solutions were previously sonicated (40 min) each time. To prepare the GONP dilution at specific ionic strength (IS), sodium chloride (NaCl, p.a. quality) was used as the background electrolyte (dissolved in DI water). All column experiments below were performed at two IS: 50 and 200 mmol/L.

1.3. Transport experiments

Transport experiments were conducted by pumping a suspension of GONPs through an acrylic column packed with clean quartz sand (Fig. 1). The acrylic column was 3 cm in diameter and 15 cm in height. Standard gravimetric methods were used to determine the sand density (1.61 g/cm^3) and a column packing porosity of 0.36 ± 0.01. The column was vertically oriented and operated in an upflow mode using a peristaltic pump at a constant Darcy's velocity of 7.5×10^{-3} cm/sec. Prior to each experiment, 20 pore volumes (PVs) of the background electrolyte solution of interest were first passed through the column to ensure that the column was fully equilibrated with this solution. Then suspension of GONPs within the same background electrolyte composition was injected into the packed column for 4 PVs (phase 1), followed by elution with GO-free solution again (phase 2). The outflow from the columns was connected by an auto fraction sampler (Huxi, CBS-A 100, Shanghai, China), and the effluent GONP concentration was monitored using UV–Vis spectrophotometer (Shimadzu, UV-2450, Kyoto, Japan) at a wavelength of 230 nm. Prior to the GONP transport experiments, the tracer (Br^-) breakthrough tests were performed to estimate the hydraulic dispersion coefficient.

In order to elucidate the influence of surfactants on GONPs transport, typical anionic (sodium dodecylbenzene sulfonate, SDBS) and non-ionic surfactants (Triton X-100) were added into the background electrolyte composition. Dispersions were prepared to have five systems per IS: no surfactant, 50% and 100% critical micelle concentration (CMC) SDBS, 50% and 100% CMC Triton X-100. The CMC for Triton X-100 and SDBS were reported to be 0.24 mmol/L (Du et al., 2013) and 963 mg/L (Godinez et al., 2013), respectively. These systems became the feeding solutions for the different experiments conducted in this study.

1.4. Mathematical modeling

The DLVO theory was used to calculate the interaction forces between GONPs and sand grains under the tested conditions. The DLVO forces consider van der Waals (VDW) attraction and electric double layer (EDL) repulsion. The total interaction energy is the sum of energies of these two interactions. In this study, the Hamaker approximate expression for a sphere-plane case (Gregory, 1981) was used for calculating the retarded VDW attractive interaction; with the assumption of constant potential at the surface, the EDL interaction was calculated by the method derived by Hogg et al. (1966). The average hydrodynamic radius and zeta potential involved into these calculations were determined by dynamic light scattering (DLS) and electrokinetic characterization measurements using ZetaSizer Nano (Malvern).

The transport process of GONPs within the saturated sand column was described by an advection–dispersion–

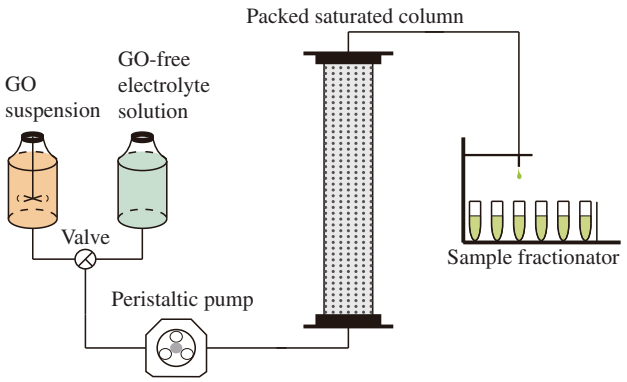

Fig. 1 – Schematic of the experimental apparatus and setup. GO: graphene oxide.

retention (ADR) model considering the combined process of Languirian dynamics blocking and depth-dependent straining. The governing equations can be written as:

$$\frac{\partial(nC)}{\partial t}+\rho\frac{\partial S}{\partial t}=nD\frac{\partial^2 C}{\partial x^2}-q\frac{\partial C}{\partial x} \quad (1)$$

$$\rho\frac{\partial S}{\partial t}=nk_{att}\psi C-k_{det}\rho S \quad (2)$$

$$\psi=\left(1-\frac{S}{S_{max}}\right)\left(\frac{d_c+x}{d_c}\right)^{-\beta} \quad (3)$$

where, n is the porosity; C (mg/L) is the concentration of GO in effluent water; ρ (g/cm^3) is the bulk density of the porous media; S (mg/g) is the solid phase concentration of GO sorbed on quartz sand; q is the flow rate; k_{att} (min^{-1}) and k_{det} (min^{-1}) are the first-order attachment and detachment coefficient, respectively; ψ is a dimensionless function to account for the combined process of Languirian dynamics blocking and depth-dependent straining (Bradford and Bettahar, 2006; Shang et al., 2013); S_{max} (mg/g) is the maximum solid phase particle concentration; d_c is the median diameter of the sand grains (d_{50}, mm); and β is an empirical dimensionless variable that controls the shape of the retention profile, Bradford et al. (2003) found an optimal value of β = 0.432, and we employed this value here.

The above model Formulations (1)–(3) were solved numerically with a finite-difference scheme for zero initial GO concentration, and pulse-input and zero-concentration-gradient boundary conditions at the column inlet and outlet, respectively. Then the solutions were fitted to GO breakthrough curves to obtain the parameters k_{att}, k_{det} and S_{max}. The effluent mass recovery rate was also calculated by integrating the BTCs, then the total deposition rates (R_d) of GONPs in columns could be estimated based upon the specified mass input of GO.

2. Results and discussion

2.1. GONPs properties

Results of the average hydrodynamic diameter and zeta potential measurements of GONPs are shown in Fig. 2. In agreement with the anticipated influence of EDL compression, the IS played a significant role on both the zeta potential and hydrodynamic diameter. The hydrodynamic diameter increased with IS, while the absolute zeta potential presented the opposite trend (less negatively), as compression of the EDL gave rise to continuous decrease in the magnitude of surface zeta potential (Lanphere et al., 2013; Akbour et al., 2013). The hydrodynamic diameter of GONPs in the dispersions containing surfactants was smaller than the one without surfactants regardless of the IS, demonstrating that surfactants allow GONPs to remain dispersed or stable. Further, the absolute zeta potential increased with concentration of surfactants, which was bound to induce stronger electrostatic repulsion forces between particles. These results were in a good agreement with the works reported by Godinez and Darnault (2011) and Villamizar et al. (2013). The enhancement of electrostatic repulsion is likely because the surfactants adsorbed to particle surface displaced the counterions and then caused expansion of the electric double layer (Sjöberg et al., 1999; Brown and Jaffé, 2001; Du et al., 2013). Interestingly, note that SDBS showed larger effect than Triton X-100 on the zeta potential and hydrodynamic diameter under the same percent CMC. For instance, at IS of 50 mmol/L, the average hydrodynamic diameter was 1447.6 nm in the presence of 50% CMC SDBS, and it was 1969.3 nm in the presence of

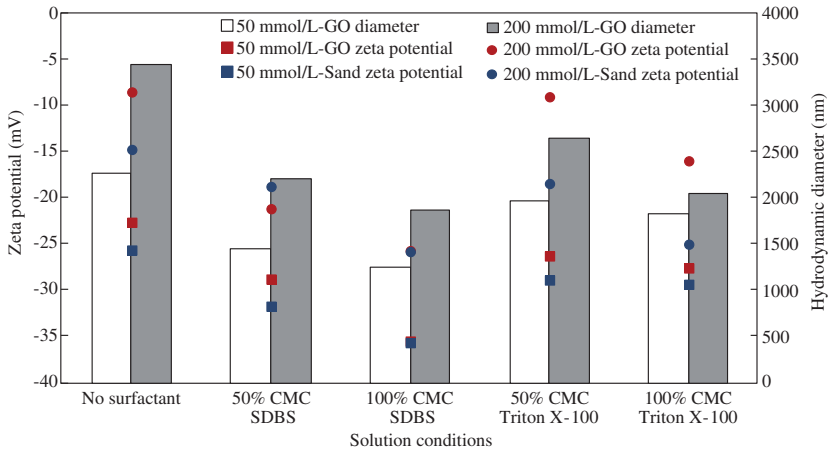

Fig. 2 – The average hydrodynamic diameter and Zeta potential of graphene oxide (GO) under experimental conditions.

50% CMC Triton X-100, while the zeta potentials were −28.8 and −26.3 mV respectively. As to sand particles, the variation of zeta potential was consistent with that of GONPs, while the sand diameter was regarded as constant (d_{50} = 0.42 mm).

In addition to electrostatic repulsion, previous studies also supposed that surfactants adsorb to the surface of particles creating steric repulsion between particles thus inhibiting interactions and preventing more aggregation which can cause an increase in particle size (Godinez and Darnault, 2011). Surfactants can form a monolayer packing on colloid (or nanoparticle) and sand surfaces by hydrogen bonding between the carboxyl surface groups (COOH) and ethylene oxide chain, and induce hydrophobic interaction (Geffroy et al., 2000; Romero-Cano et al., 2002). This hydrophobic interaction affects the surfactant sorption significantly. The sorption of surfactants onto both colloidal and sand surfaces increases steric repulsion between colloids and collectors. This steric effect was dependent on the thickness of the electric double layer (Debeye length) and the polymer chain length, and steric effect only works when the chains of the sorbed surfactant layer could extend beyond the EDL (Brown and Jaffé, 2001). Actually, the Debeye lengths at IS of 50 and 200 mmol/L were 1.23 and 0.68 nm according to the calculated method described by Qi et al. (2014), while the chain lengths of SDBS and Triton X-100 were 0.35 and 0.43 nm that were calculated according to Shon et al. (2006). It was obvious that the chain of both surfactants remained well within the electric double layer. In addition, the chain length of SDBS was shorter than that of Triton X-100, but displayed significant effect on preventing aggregation. It appeared that steric effects are insignificant for our experimental system, and electrostatic interactions dominated the particle interactions. Therefore, the negatively charged SDBS should be more effective to disperse the GONPs with the same charge compared to the neutral Triton X-100. Hua et al. (2009) also demonstrated such a difference between the SDBS and Triton X-100, and attributed it to their opposite surface charge.

2.2. DLVO interaction energies

DLVO interaction energy (Φ) profiles for different electrolyte solutions are plotted as a function of separation distance in Fig. 3. The calculated energy barriers were too large, >200 k_BT (where k_B is the Boltzmann constant and T is Kelvin temperature) to overcome. Consequently GONPs hardly deposited into the primary energy minimum (Liu et al., 2013a; Shang et al., 2013). The energy barrier decreased with increasing IS, indicating that there were greater repulsive forces upon the approach to the sand surface at IS of 50 mmol/L compared to 200 mmol/L. Similarly, the presence and concentration of surfactants also raised the height of energy barrier, and then prevented the deposition of GONPs into the primary energy minimum more firmly. It has been also reported in the literatures that secondary energy minima played a critical role in the particle aggregation and deposition (Redman et al., 2004; Kuznar and Elimelech, 2007; Mesticou et al., 2014). The DLVO interaction energy profiles confirmed this by replotting on a different scale (Fig. 3c and d). It showed two secondary minimum wells at −0.0956 and −0.9315 k_BT for the IS of 50 and 200 mmol/L in the absence of surfactants, respectively. The increase of IS and decrease of concentration of surfactants deepened the secondary minimum wells distinctly, thus higher IS and lower surfactant concentration could enhance the secondary minimum deposition relatively. Compared to Triton X-100 at the same percent CMC and IS, the profiles in the case of solutions containing SDBS displayed higher primary energy barriers and lower secondary minimum wells, which gave a further indication that Triton X-100 contributed to the secondary minimum attachment more effectively.

2.3. Influence of ionic strength on GO transport

Particle breakthrough curves (BTCs) obtained at experimental conditions were presented in Fig. 4, and the best-fit transport parameters in model were listed in Table 1 (the numerical model described all the experimental breakthrough curves very well, $R^2 > 0.90$). In the figure, the normalized effluent GONP concentration C/C_0 was plotted as a function of pore volume. The deposition of GONPs increased (C/C_0 decreased) with increasing IS both in the presence or absence of surfactants. The maximum of C/C_0 at 50 mmol/L was 1.61–3.16 times as those at 200 mmol/L, while the average deposition rates R_d were 39.28% and 70.55% respectively. This trend of decreasing breakthrough with increasing IS follows the DLVO calculation, suggesting that electrostatic interactions were the main mechanisms controlling the transport of GONPs. In principle, when the concentration of NaCl in the solution increased, the diffuse double layers were compressed causing a reduction in the repulsive electrostatic double-layer forces and increase in the particle deposition rate (Knappett et al., 2008; Rahman et al., 2013). The variations of k_{att} and S_{max} in modeling verified this trend quantitatively, indicating that GONPs were less mobile in higher IS. It was quite consistent with former studies on GO transport (Feriancikova and Xu, 2012; Lanphere et al., 2013).

2.4. Effect of no surfactants vs. surfactants on GONP transport

By comparison of particle BTCs obtained in the presence of surfactant with BTCs measured without the addition of surfactant (Fig. 4), it was clear that the presence and concentration of surfactant could enhance the GONP transport in sand column regardless of the surfactant type. The total deposition rates R_d were 50.84% and 79.41% in the absence of surfactants at 50 mmol/L and 200 mmol/L respectively, while they reduced to 32.48% and 59.54% in the presence of 100% CMC SDBS, and 36.01% and 64.31% in the presence of 100% CMC Triton X-100. It was additionally observed that the increase of GONP mobility translated by increasing percent CMC (from 50% to 100% CMC) was relatively less obvious at 50 mmol/L than that at 200 mmol/L. We supposed that this phenomenon attributed to the main particle retention mechanisms in porous media: attachment and straining. As described in previous literatures, the surfactants contributed unambiguously to the repulsion forces and inhibited the particle aggregation and attachment under a wide range of IS (Tufenkji and Elimelech, 2005). However, the influence of surfactants on straining was not significant at lower IS compared with higher IS (Du et al., 2013). Actually, the straining process was undoubtedly much more remarkable under higher IS due to the electrostatic double

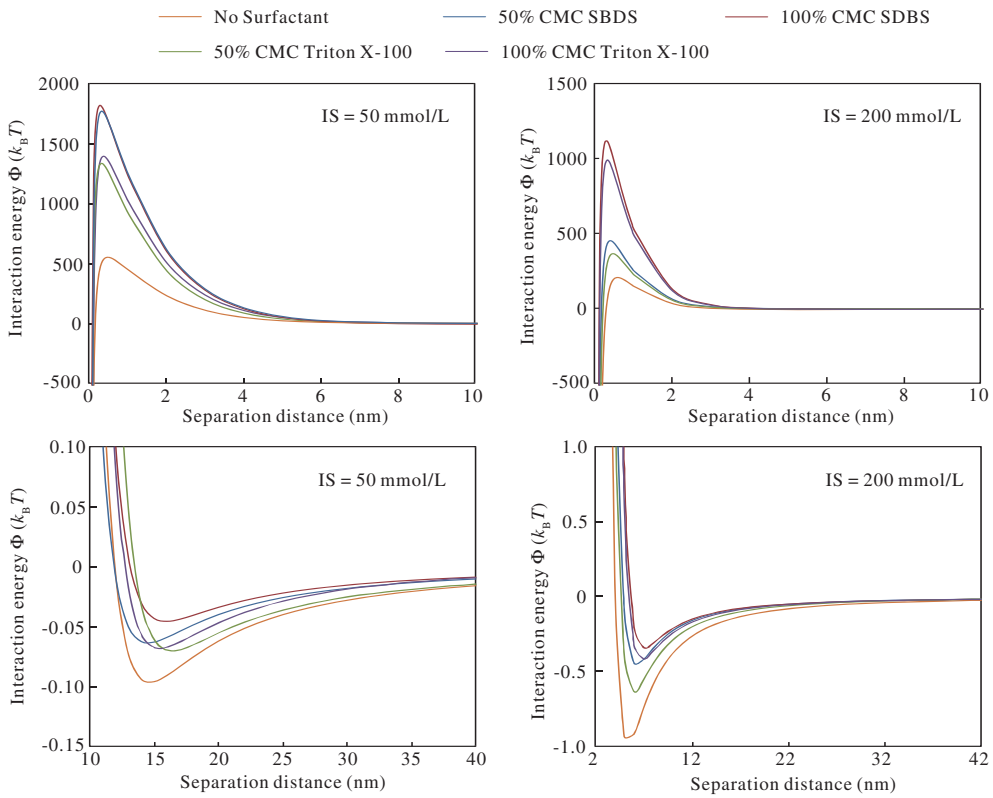

Fig. 3 – Derjaguin–Landau–Verwey–Overbeek (DLVO) energy profiles between the graphene oxide and sand particles. (a) and (c), IS = 50 mmol/L; (b) and (d), IS = 200 mmol/L. IS is short for ionic strength.

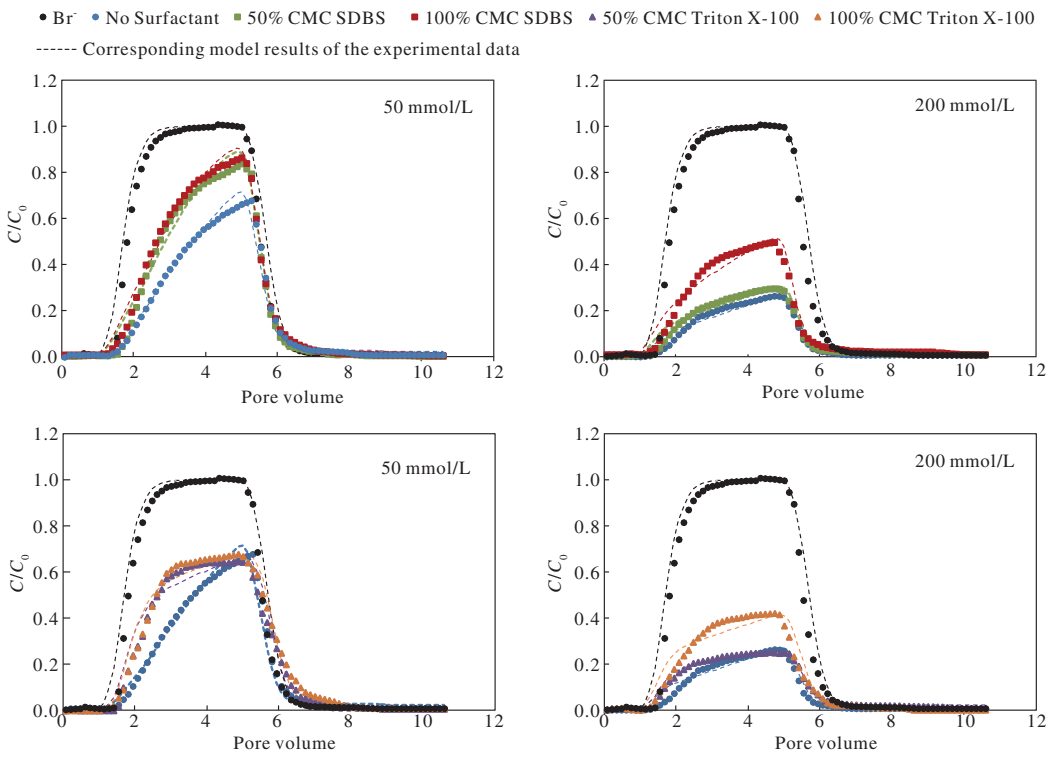

Fig. 4 – Observed and modeled breakthrough curves of the tracer (Br^-) and graphene oxide in columns.

Table 1 – Summary of experimental conditions and model results. SDBS: sodium dodecylbenzene sulfonate; CMC: critical micelle concentration.

Ionic strength (mmol/L)	Dispersion system	R_d	k_{att} (min^{-1})	k_{det} (min^{-1})	S_{max} (mg/g)	R^2
50	No surfactant	50.84%	1.374	0.002	0.345	0.98
50	50% CMC SDBS	36.99%	0.875	0.001	0.219	0.99
50	100% CMC SDBS	32.48%	0.847	0.002	0.202	0.99
50	50% CMC Triton X-100	40.06%	1.280	0.003	0.302	0.96
50	100% CMC Triton X-100	36.01%	1.170	0.006	0.299	0.95
200	No surfactant	79.41%	1.522	0.001	1.316	0.96
200	50% CMC SDBS	74.51%	1.101	0.001	1.202	0.97
200	100% CMC SDBS	59.54%	0.845	0.001	0.894	0.93
200	50% CMC Triton X-100	74.98%	1.365	0.002	1.296	0.98
200	100% CMC Triton X-100	64.31%	1.187	0.001	1.023	0.96

layer compression and subsequent particle agglomeration (increase of particle size) (Bradford et al., 2007; Chowdhury et al., 2013; Wu et al., 2013). Taken together, influence of surfactants on enhancement of GONPs transport was therefore rather limited at lower IS (50 mmol/L), and the increase of surfactant concentration could not obtain apparent effect.

2.5. *Influence of anionic surfactants vs. non-ionic surfactants on GONP transport*

To investigate the effectiveness of the type of surfactant on the GONP transport through saturated sand media, the BTCs of several scenarios that involved specific concentration (percent CMC) of SDBS and Triton X-100 were compared based on IS variation (Fig. 4). It was interesting to see that the GONP transport was surfactant type dependent. p R_d, k_{att} and S_{max} in the cases of SDBS were lower than those in cases of Triton X-100 under the same IS and percent CMC conditions. Although there were not considerable differences in magnitude, the consistency and regularity of the changes of these parameters still could suggest that SDBS was more effective to facilitate GONP transport than Triton X-100 in our experimental conditions. This was in agreement with the DLVO profile analysis in Section 2.2, and supported with the observations by Hua et al (2009), in which, SDBS was more efficient than Triton X-100 to enhance leaching of anionic pesticide.

Moreover, the steady state portion of the particle BTCs (after 2.5–3.5 PVs injection) was considerably more flat when surfactants were added, particularly in the cases of Trion X-100. Since the influent particle concentration in all experiments was comparable, flattening of the BTCs could be contributed to elimination of particle blocking (Tufenkji and Elimelech, 2005; Du et al., 2013; Kasel et al., 2013). It was supposed to be that blocking occurs when previously deposited particles hinder subsequent deposition and is characterized by a continual increase in the effluent suspended particle concentration (Nascimento et al., 2006; Porubcan and Xu, 2011). Firstly, adsorbed surfactants masked certain surface heterogeneity of both GONPs and sand, thus eliminating the favorable deposition sites and reducing the extent of "fast" deposition at the initial stage, which could contribute to flatten the BTCs. Secondly, compared to Trion X-100, SDBS, as anionic surfactants, would make the sand and particle surface more negative (affirmed by Zeta potential measurement in Section 2.1), consequently enhanced the repulsion force between particles and promoted blocking effects. The variations of the blocking parameters S_{max} in Table 1 also verified this law. The S_{max} was smaller in the case of SDBS than that of Trion X-100.

It's also worth noting that there were no size exclusion phenomenon in our experiments according to the coincident time of GONPs and tracer to reach the column outlet in BTCs. And the C/C_0 of GONPs quickly reached 0 after elution by 6 PVs GO-free solution, suggesting that the release of immobilized GONPs could be negligible under the same IS. That's why the fitted values of k_{det} in the model were quite small.

3. Conclusions

This study demonstrated that the mobility of GONPs in saturated porous media was dependent upon the presence and concentration of the surfactants. Higher surfactant concentration could enhance the GONP mobility by influencing the secondary minimum deposition. The total deposition rates R_d were even down by more than 6–36% in the presence of surfactants in our experiments. It was also interesting to see that the GONP transport was surfactant type dependent. SDBS was more effective to facilitate GONP transport than Triton X-100 under the same IS and percent CMC conditions, displaying a considerable potential to reduce the R_d by 0.6–9.8%. Findings from this study also showed that the mathematical model considering the combined process of Languirian dynamics blocking and depth-dependent straining could be used to simulate the transport behavior of GONPs in soil and groundwater system.

Acknowledgments

This work was financially supported by National Natural Science Foundation of China (NSFC NO. 41302196 and 51238001). It was also supported by the Fundamental Research Funds for the Central Universities (NO. 14QNJJ026).

REFERENCES

Adak, A., Bandyopadhyay, M., Pal, A., 2005. Removal of anionic surfactant from wastewater by alumina: a case study. Colloids Surf. A Physicochem. Eng. Asp. 254 (1-3), 165–171.

Ahmed, F., Rodrigues, D.F., 2013. Investigation of acute effects of graphene oxide on wastewater microbial community: a case study. J. Hazard. Mater. 256–257, 33–39.
Akbour, R.A., Amal, H., Ait-Addi, A., Douch, J., Jada, A., Hamdani, M., 2013. Transport and retention of humic acid through natural quartz sand: influence of the ionic strength and the nature of divalent cation. Colloids Surf. A Physicochem. Eng. Asp. 436, 589–598.
Bao, C.L., Song, L., Xing, W.Y., Yuan, B.H., Wilkie, C.A., Huang, J.L., et al., 2012. Preparation of graphene by pressurized oxidation and multiplex reduction and its polymer nanocomposites by masterbatch-based melt blending. J. Mater. Chem. 22 (13), 6088–6096.
Bradford, S.A., Bettahar, M., 2006. Concentration dependent transport of colloids in saturated porous media. J. Contam. Hydrol. 82 (1-2), 99–117.
Bradford, S.A., Simunek, J., Bettahar, M., van Genuchten, M.T., Yates, S.R., 2003. Modeling colloid attachment, straining, and exclusion in saturated porous media. Environ. Sci. Technol. 37 (10), 2242–2250.
Bradford, S.A., Torkzaban, S., Walker, S.L., 2007. Coupling of physical and chemical mechanisms of colloid straining in saturated porous media. Water Res. 41 (13), 3012–3024.
Brown, D.G., Jaffé, P.R., 2001. Effects of nonionic surfactants on bacterial transport through porous media. Environ. Sci. Technol. 35 (19), 3877–3883.
Chowdhury, I., Duch, M.C., Mansukhani, N.D., Hersam, M.C., Bouchard, D., 2013. Colloidal properties and stability of graphene oxide nanomaterials in the aquatic environment. Environ. Sci. Technol. 47 (12), 6288–6296.
Dreyer, D.R., Park, S., Bielawski, C.W., Ruoff, R.S., 2010. The chemistry of graphene oxide. Chem. Soc. Rev. 39 (1), 228–240.
Du, Y.C., Shen, C.Y., Zhang, H.Y., Huang, Y.F., 2013. Effects of flow velocity and nonionic surfactant on colloid straining in saturated porous media under unfavorable conditions. Transp. Prous. Med. 98 (1), 193–208.
Feriancikova, L., Xu, S.P., 2012. Deposition and remobilization of graphene oxide within saturated sand packs. J. Hazard. Mater. 235–236, 194–200.
Geffroy, C., Cohen Stuart, M.A., Wong, K., Cabane, B., Bergeron, V., 2000. Adsorption of nonionic surfactants onto polystyrene: kinetics and reversibility. Langmuir 16 (16), 6422–6433.
Godinez, I.G., Darnault, C.J.G., 2011. Aggregation and transport of nano-TiO_2 in saturated porous media: effects of pH, surfactants and flow velocity. Water Res. 45 (2), 839–851.
Godinez, I.G., Darnault, C.J., Khodadoust, A.P., Bogdan, D., 2013. Deposition and release kinetics of nano-TiO_2 in saturated porous media: effects of solution ionic strength and surfactants. Environ. Pollut. 174, 106–113.
Gregory, J., 1981. Approximate expressions for retarded van der Waals interaction. J. Colloid Interface Sci. 83 (1), 138–145.
Hennebert, P., Avellan, A., Yan, J.F., Aguerre-Chariol, O., 2013. Experimental evidence of colloids and nanoparticles presence from 25 waste leachates. Waste Manag. 33 (9), 1870–1881.
Hogg, R., Healy, T.W., Fuerstenau, D.W., 1966. Mutual coagulation of colloidal dispersions. Trans. Faraday Soc. 62, 1638–1651.
Hua, R.M., Spliid, N.H., Heinrichson, K., Laursen, B., 2009. Influence of surfactants on the leaching of bentazone in a sandy loam soil. Pest Manag. Sci. 65 (8), 857–861.
Ju-Nam, Y., Lead, J.R., 2008. Manufactured nanoparticles: an overview of their chemistry, interactions and potential environmental implications. Sci. Total Environ. 400 (1-3), 396–414.
Kasel, D., Bradford, S.A., Šimůnek, J., Heggen, M., Vereecken, H., Klumpp, E., 2013. Transport and retention of multi-walled carbon nanotubes in saturated porous media: effects of input concentration and grain size. Water Res. 47 (2), 933–944.
Knappett, P.S., Emelko, M.B., Zhuang, J., McKay, L.D., 2008. Transport and retention of a bacteriophage and microspheres in saturated, angular porous media: effects of ionic strength and grain size. Water Res. 42 (16), 4368–4378.
Kuznar, Z.A., Elimelech, M., 2007. Direct microscopic observation of particle deposition in porous media: role of the secondary energy minimum. Colloid. Surf. A-Physicochem. Eng. Asp. 294 (1-3), 156–162.
Lanphere, J.D., Luth, C.J., Walker, S.L., 2013. Effects of solution chemistry on the transport of graphene oxide in saturated porous media. Environ. Sci. Technol. 47 (9), 4255–4261.
Lin, D., Liu, N., Yang, K., Xing, B., Wu, F., 2010. Different stabilities of multiwalled carbon nanotubes in fresh surface water samples. Environ. Pollut. 158 (5), 1270–1274.
Liu, L., Gao, B., Wu, L., Morales, V.L., Yang, L.Y., Zhou, Z.H., et al., 2013a. Deposition and transport of graphene oxide in saturated and unsaturated porous media. Chem. Eng. J. 229, 444–449.
Liu, L., Gao, B., Wu, L., Yang, L.Y., Zhou, Z.H., Wang, H., 2013b. Effects of pH and surface metal oxyhydroxides on deposition and transport of carboxyl-functionalized graphene in saturated porous media. J. Nanoparticle Res. 15 (11), 2079–2086.
Mesticou, Z., Kacem, M., Dubujet, P., 2014. Influence of ionic strength and flow rate on silt particle deposition and release in saturated porous medium: experiment and modeling. Transp. Porous Media 103 (1), 1–24.
Nascimento, A.G., Tótola, M.R., Souza, C.S., Borges, M.T., Borges, A.C., 2006. Temporal and spatial dynamics of blocking and ripening effects on bacterial transport through a porous system: a possible explanation for CFT deviation. Colloids Surf. B: Biointerfaces 53 (2), 241–244.
Novikov, A.P., Kalmykov, S.N., Utsunomiya, S., Ewing, R.C., Horreard, F., Merkulov, A., et al., 2006. Colloid transport of plutonium in the far-field of the Mayak Production Association. Science 314 (5799), 638–641.
Petosa, A.R., Jaisi, D.P., Quevedo, I.R., Elimelech, M., Tufenkji, N., 2010. Aggregation and deposition of engineered nanomaterials in aquatic environments: role of physicochemical interactions. Environ. Sci. Technol. 44 (17), 6532–6549.
Porubcan, A.A., Xu, S.P., 2011. Colloid straining within saturated heterogeneous porous media. Water Res. 45 (4), 1796–1806.
Qi, Z.C., Zhang, L.L., Wang, F., Hou, L., Chen, W., 2014. Factors controlling transport of graphene oxide nanoparticles in saturated sand columns. Environ. Toxicol. Chem. 33 (5), 998–1004.
Rahman, T., George, J., Shipley, H.J., 2013. Transport of aluminum oxide nanoparticles in saturated sand: effects of ionic strength, flow rate, and nanoparticle concentration. Sci. Total Environ. 463–464, 565–571.
Redman, J.A., Walker, S.L., Elimelech, M., 2004. Bacterial adhesion and transport in porous media: role of the secondary energy minimum. Environ. Sci. Technol. 38 (6), 1777–1785.
Romero-Cano, M.S., Martín-Rodríguez, A., de las Nieves, F.J., 2002. Electrokinetic behaviour of polymer colloids with adsorbed Triton X-100. Colloid Polym. Sci. 280 (6), 526–532.
Saito, T., Suzuki, Y., Mizuno, T., 2013. Size and elemental analyses of nano colloids in deep granitic groundwater: implications for transport of trace elements. Colloid. Surf. A-Physicochem. Eng. Asp. 435, 48–55.
Shang, J.Y., Liu, C.X., Wang, Z.M., 2013. Transport and retention of engineered nanoporous particles in porous media: effects of concentration and flow dynamics. Colloid. Surf. A-Physicochem. Eng. Asp. 417, 89–98.
Shon, H.K., Kim, S.H., Erdei, L., Vigneswaran, S., 2006. Analytical methods of size distribution for organic matter in water and wastewater. Korean J. Chem. Eng. 23 (4), 581–591.
Sjöberg, M., Bergström, L., Larsson, A., Sjöström, E., 1999. The effect of polymer and surfactant adsorption on the colloidal stability and rheology of kaolin dispersions. Colloid. Surf A-Physicochem. Eng. Asp. 159 (1), 197–208.
Srivastava, R.K., Wang, X., Kumar, V., Srivastava, A., Singh, V.N., 2014. Synthesis of benzimidazole-grafted

graphene oxide/multi-walled carbon nanotubes composite for supercapacitance application. J. Alloys Compd. 612, 343–348.
Tkachenko, N.H., Yaremko, Z.M., Bellmann, C., Soltys, M.M., 2006. The influence of ionic and nonionic surfactants on aggregative stability and electrical surface properties of aqueous suspensions of titanium dioxide. J. Colloid Interface Sci. 299 (2), 686–695.
Tufenkji, N., Elimelech, M., 2005. Breakdown of colloid filtration theory: role of the secondary energy minimum and surface charge heterogeneities. Langmuir 21 (3), 841–852.
Villamizar, L.C., Lohateeraparp, P., Harwell, J.H., Resasco, D.E., Shiau, B.J., 2013. Dispersion stability and transport of nanohybrids through porous media. Transp. Porous. Med. 96 (1), 63–81.
Wang, K., Ruan, J., Song, H., Zhang, J.L., Wo, Y., Guo, S.W., et al., 2011. Biocompatibility of graphene oxide. Nanoscale Res. Lett. 6 (1), 1–8.
Wu, L., Liu, L., Gao, B., Muñoz-Carpena, R., Zhang, M., Chen, H., et al., 2013. Aggregation kinetics of graphene oxides in aqueous solutions: experiments, mechanisms, and modeling. Langmuir 29 (49), 15174–15181.
Zhang, H., Huang, H., Lin, Z.H., Su, X.G., 2014. A turn-on fluorescence-sensing technique for glucose determination based on graphene oxide–DNA interaction. Anal. Bioanal. Chem. 406 (27), 6925–6932.